Water Resources Management
https://doi.org/10.1007/s11269-024-03917-6

Comparison of Hydrological Modeling, Artificial Neural Networks and Multi-Criteria Decision Making Approaches for Determining Flood Source Areas

Erfan Mahmoodi[1] · Mahmood Azari[1] · Mohammad Taghi Dastorani[1] · Aryan Salvati[2]

Received: 3 January 2024 / Accepted: 15 June 2024

Abstract
Flood risk management is a critical task which necessitates flood forecasting and identifying flood source areas for implementation of prevention measures. Hydrological models, multi-criteria decision models (MCDM) and data-driven models such as the Artificial Neural Networks (ANN) have been used to identify flood source areas within a watershed. The aim of this study was to compare the results of hydrological modeling, MCDM and the ANN approaches in order to identify and prioritize flood source areas. The study results show that the classification results of the hydrological model and the ANN have a significant correlation. The correlation between the TOPSIS method with the hydrological model indicate no meaningful correlation. Since the ANN model has simulated the HEC-HMS classifications very accurately, it can be a good substitute for the hydrological models in watersheds with limited data.

Keywords Flood hazard susceptibility · Hydrological modeling · Flood source areas · ANN

1 Introduction

Floods have been one of the most prevalent (47%) climate-related disasters in the last two decades; more hazardous than landslides, earthquakes, and volcanoes, affecting 2.3 billion people and causing the third biggest amount of economic damage (662 billion USD) according to the CRED and UNISDR analysis (Bolt et al. 2013; CrED 2015). Floods are expected to increase in frequency and intensity in the coming years due to the rising sea levels and heavy rainfall events (Wang et al. 2015). As a result, flood management and risk reduction are critical, which necessitate flood forecasting and identifying flood source areas for implementation of flood control and prevention measures (Hong et al. 2018). The intention of flood risk assessment is to arrive at an accurate risk level. The multivariate and nonlinear relation between indicators and risk levels is the fundamental issue with this procedure (Solin and

✉ Mahmood Azari
m.azari@um.ac.ir

[1] Department of Range and Watershed Management, Faculty of Natural Resources and Environment, Ferdowsi University of Mashhad, Mashhad, Iran

[2] Department of Arid and Mountainous Regions Reclamation, Faculty of Natural Resources, University of Tehran, Karaj, Iran

Skubincan 2013). One of the most important tasks in flood control is identifying the best methods for locating flood source areas (FSA) within a watershed in order to improve flood prevention techniques (Singh et al. 2021). In response to this need, many systematic methods such as hydrological models (Abdulkareem et al. 2018; Dehghanian et al. 2019; Maghsood et al. 2019; Soomro et al. 2022), GIS-based methods (Cabrera and Lee 2019; Hong and Abdelkareem 2022; Mukherjee and Singh 2020; Osei et al. 2021), remote sensing methods (Sadiq et al. 2022; Sharma et al. 2019; Syifa et al. 2019), multi-criteria decision methods (Ajjur and Mogheir 2020; dos Santos et al. 2023; Hadian et al. 2022; Pham et al. 2021; Roy et al. 2021; Solaimani et al. 2023), and machine learning and data mining methods (Costache et al. 2022; Ghobadi and Ahmadipari 2024; Ha and Kang 2022; Islam et al. 2023; Luu et al. 2021; Rahman et al. 2021; Zohourian and Hosseini 2023) have been used.

Hydrological models are used to simulate the hydrological cycle and facilitate the understanding and simulation of complex hydrological processes. Hydrological models can be based on physical principles, empirical relationships, or a combination of both (Beven 2001). They are typically used for water resources management (Loucks and Van Beek 2017; Xu et al. 2023), flood forecasting (Koya et al. 2023; Pappenberger et al. 2006), drought analysis (Van Loon 2015), and environmental impact assessment (Dong et al. 2023; Viviroli et al. 2007). However, hydrological models require extensive data inputs and calibration, which can be time-consuming. Model accuracy can be affected by uncertainties in input data, model structure, and simplifications of complex processes, and interpretation and application of the results may be limited due to model complexity and uncertainties (Beven 2001). Therefore, hydrological models are not sufficient for flood hazard studies in ungauged catchments. A valuable tool for overcoming this limitation in hydrological modeling is the use of multi-criteria decision models and machine learning algorithms.

Multi-criteria decision methods (MCDM) are decision-making tools used for evaluating and comparing alternatives based on multiple criteria or objectives (Saaty 1980). These methods aim to find the best or optimal solution among a set of alternatives by considering multiple criteria, which can be quantitative or qualitative in nature (Belton and Stewart 2002). Some commonly used MCDM methods in hydrology include Analytic Hierarchy Process (AHP) (Wijesinghe et al. 2023), Technique for Order of Preference by Similarity to Ideal Solution (TOPSIS) (Hwang and Yoon 1981; Mitra and Das 2023), and Preference Ranking Organization Method for Enrichment Evaluations (PROMETHEE) (Brans et al. 2005; Dadrasajirlou et al. 2023). Multi-criteria decision methods provide a structured approach to consider multiple criteria and objectives in decision-making (Saaty 1980). Multi-criteria decision models often cost less and are easier to implement in hydrological applications than other types of conceptual/physical rainfall-runoff models (Belton and Stewart 2002).

Data-driven models, such as the ANNs models, have also been developed to simulate rainfall-runoff processes in flow prediction because the runoff process is a complex, nonlinear process. The ANNs are computational models inspired by the structure and function of biological neural networks, such as the human brain (McCulloch and Pitts 1943). These models have the ability to capture complex nonlinear relationships and can be trained using historical hydrological data to simulate or predict hydrological variables. They are used in hydrology for various tasks, including stream flow forecasting (Liu et al. 2023), rainfall-runoff modeling (Dawson and Wilby 2001; Mohseni and Muskula 2023), and groundwater level prediction (Bai and Tahmasebi 2023). The ANNs learn from input data through a process called training, where the network adjusts its parameters to minimize the difference between predicted and actual outputs. The ANNs require a large amount of training data, and data quality and representativeness are crucial for model performance. Interpreting the internal workings of the ANNs can be challenging, limiting their use in decision-making and model understanding (Dawson and Wilby 2001).

Since the use of hydrological models in determining flood prone areas is associated with many challenges, the application of data-driven methods and MCDM methods have received more attention in recent years. However, a comprehensive evaluation and comparison of the results attained from these three approaches has not been provided yet. The novelty of this research is to compare the accuracy of hydrological modeling, multi-criteria decision-making and the ANN approaches for identifying and prioritizing flood source areas. For this purpose, hydrological process and flood generation simulated by HEC-HMS model and the results of hydrological model used for training the ANN models. Also, using morphometric parameters in a MCDM model (TOPSIS), sub-basins were prioritized based on flood generation.

2 Materials and Methods

2.1 Study Area

The study area of this research is the upper Darungar watershed in northeastern Iran, spans the latitudes of 37°17′56" N to 37°40′50" N and the longitudes of 58°11′17" E to 58°41′44" E. (Fig. 1). The Darungar watershed covers an area of 941.1 km^2. Its lowest elevation is 990 m above sea level, while its maximum height is 2922 m above sea level. The research area has a cold, semi-arid climate according to the Emberger method, with 304.2 mm of annual rainfall and average yearly temperature is 12.1 degrees Celsius as well. The basin's topography is rough and abrupt, with a slope of 63.8 percent on average. Sandstone and limestone make up the majority of the geology in the study region. Rangelands, which make up 39 percent of the total area and low dense forest, which cover 21.1 percent, are the predominant land-use types in the watershed.

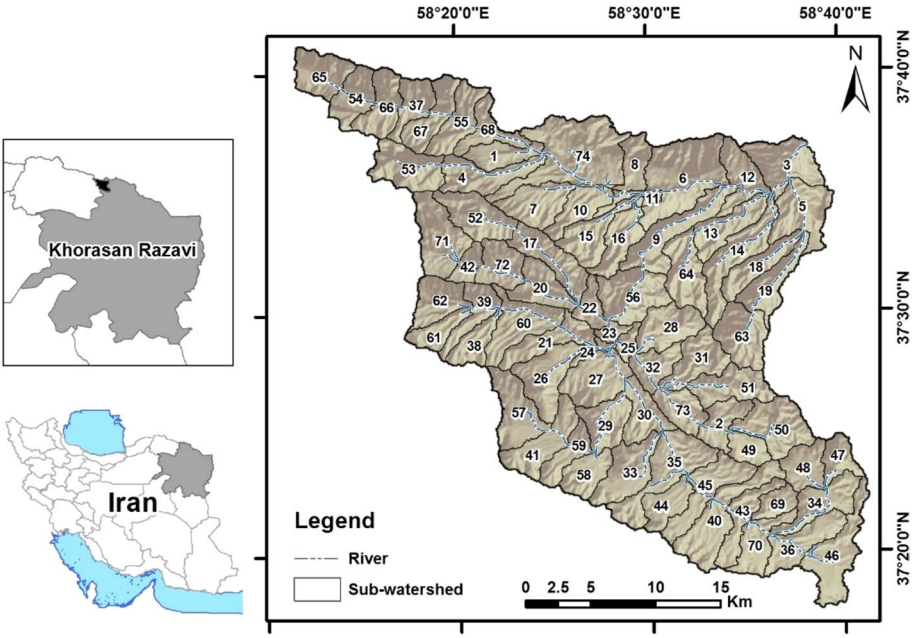

Fig. 1 Location of study area in Iran

2.2 Data

2.2.1 Rainfall Runoff Data

In this study, appropriate rainfall runoff events were selected through examining the flood hydrographs and relevant hyetographs. Due to the lack of sufficient data for sub-basin s, the data of 6 flood events available in the Iranian Water Resources Management Company at the main outlet were used to calibrate and validate the HEC-HMS model (Table 1). Rainfall data of the meteorological stations were received from the National Meteorological Organization.

2.2.2 Digital Elevation Model (DEM)

The DEM provides a three-dimensional view of the earth's surface to investigate hydrological processes. DEM of the Darungar watershed with a resolution of 30 m was acquired from the US Geological Survey (USGS) website. The DEM data was subsequently processed using the HEC-GeoHMS in ArcGIS 10.2 interface (Fig. 2b). Also, the DEM was used for creating slope map of the watershed (Fig. 2c). The slope has a direct relationship with the infiltration of runoff. The higher the slope, the lower the infiltration depth and the higher the runoff.

2.2.3 Land Use /Land Cover data (LULC)

Different LUs have different permeability of runoff. For example, dense forests have a higher permeability than other LULCs (Bonell et al. 2010). In this study, the LU map including 10 groups (Table 2) was achieved from Iran's Natural Resources and Watershed Management Organization (Fig. 2d).

2.2.4 Soil Data

Soils are classified by the Natural Resource Conservation Service into four Hydrologic Soil Groups based on the soil's runoff potential (Bailey 1976). Hydrological groups have an important effect in predicting floods through runoff penetration. The information related to soil hydrological groups was obtained from Iran's Natural Resources and Watershed Management Organization (Fig. 2e). Hydrological groups B, C, and D occupy 29.5, 65.5, and 5 percent of the studied area, respectively.

Table 1 Flood events which used for calibration and validation of HEC-HMS

Flood event	Date	Peak flow(m^3/s)	Peak time
1	May 11,1991	49.2	16:00
2	May 13,1992	74.3	10:00
3	Jun 5,1992	92.6	1:00
4	Feb 21,1999	88.4	10:00
5	Jun 8,1992	110.6	16:30
6	May 4,2002	58	0:00

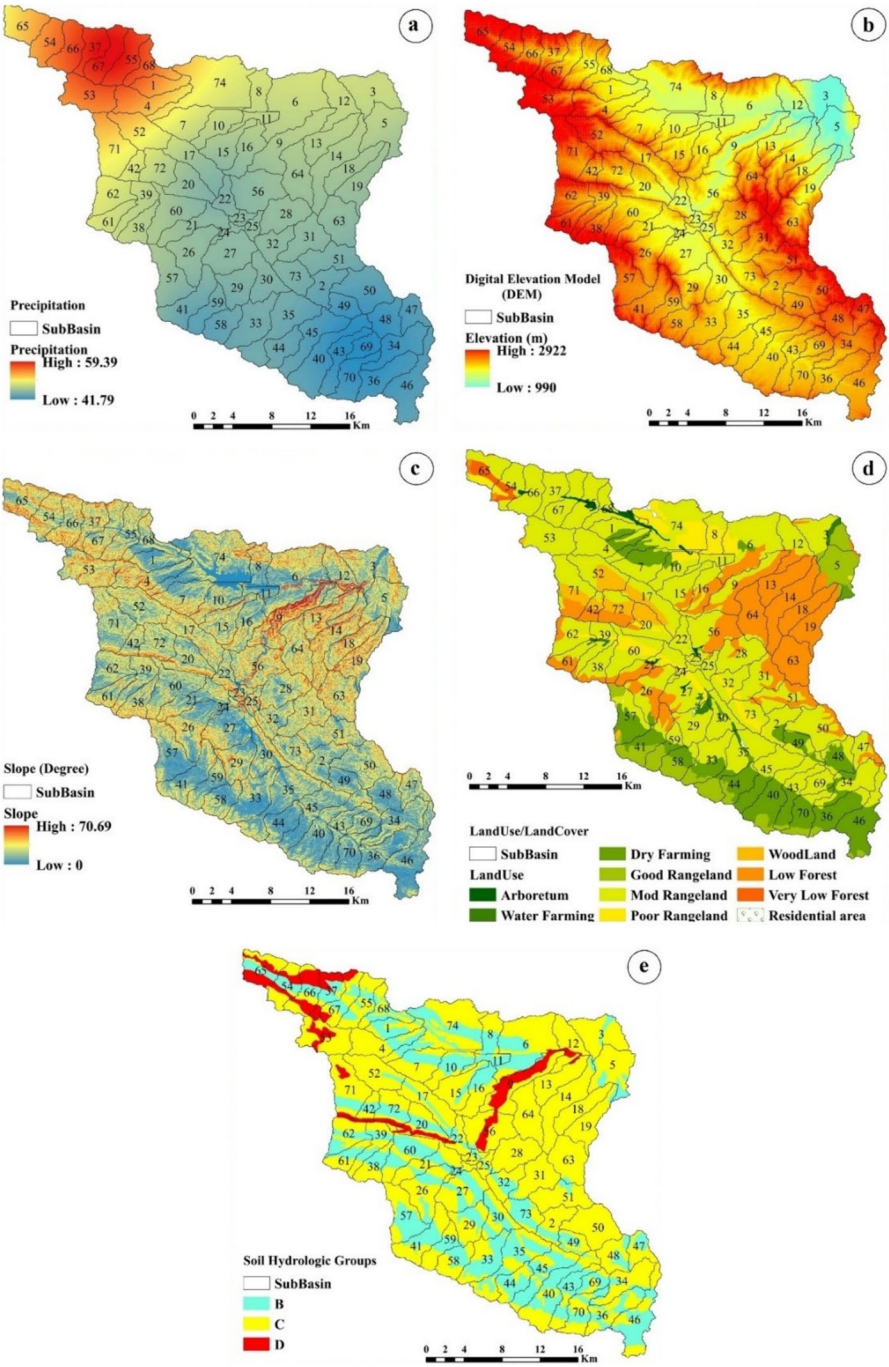

Fig. 2 Flood conditioning factors maps: (**a**) Precipitation map, (**b**) Digital Elevation Model (DEM), (**c**) Slope map, (**d**) Land use/Land cover map and (**e**) Soil hydrologic map

Table 2 The area of different LULC classes in the study area

LULC	Area (km^2)	Percent%
Mod Rangeland	485.5	52.5%
Low Forest	179.8	19.1%
Dry Farming	126.2	13.4%
Good Rangeland	52.7	5.6%
Poor Rangeland	52.3	5.5%
Wood Land	26	2.8%
Arboretum	6.5	0.69%
Very Low Forest	6.1	0.65%
Water Farming	6	0.64%
Residential area	1.2	0.12%

2.2.5 Morphometric Data

Morphometric data used in the MCDM approach included 11 morphometric parameters which were divided into linear parameters (Drainage density(Dd), Stream length(Li), Drainage texture(T), Bifurcation ratio(Br), and Stream frequency(Fs)) and shape parameters (Basin Elongation(E), Compactness index(Cc), Circularity Ratio(Rc), Form Factor(FF), Relief ratio(Rr), and Ruggedness number(Rn)). Linear parameters are directly related to runoff generation and shape parameters are inversely related to creating runoff. Table 1S shows the morphometric parameters and their values for the 74 sub-basins of Darungar Basin.

2.2.6 Topographic Wetness Index (TWI)

The TWI quantifies changes in soil moisture according to the morphometric changes of the earth's surface and can be used to identify soil saturation areas (Beven 2011). TWI values are calculated according to Eq. 1 and are shown in Fig. 3a.

$$TWI = Ln\left(\frac{A_s}{tan\beta}\right) \tag{1}$$

2.2.7 Terrain Ruggedness Index (TRI)

TRI is an important factor in flood event severity. This index has an inverse relationship with the probability of flooding, so that the occurrence of a higher probability of flooding is related to a lower TRI value (Islam et al. 2021). In this study, a TRI map with a value between 0.009 and 0.943 was prepared in GIS (Fig. 3b).

2.3 HEC-HMS Model

The HEC-HMS model is a physically based and conceptually semi-distributed model which was developed to simulate rainfall-runoff processes in a variety of geographic locations, from big river basin to small urban and natural watershed. In this study, 50-year rainfall were calculated using rainfall frequency analysis of long-term annual

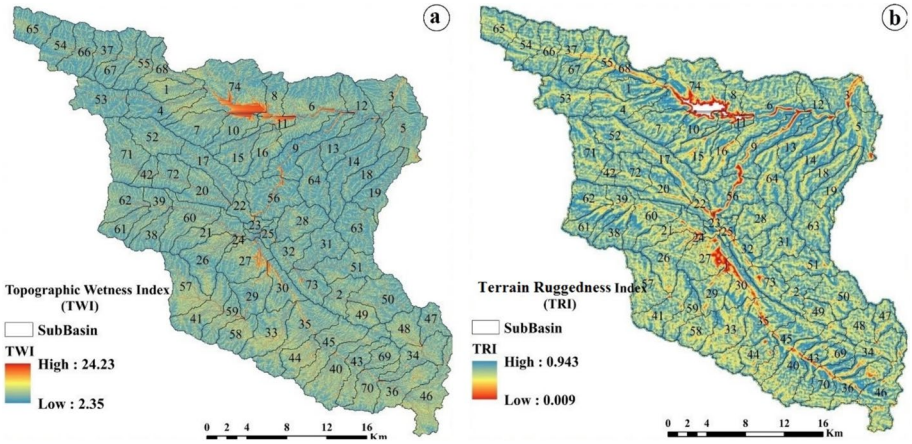

Fig. 3 Maps of (**a**) Topographic Wetness Index (TWI) and (**b**) Train Roughness Index (TRI)

maximum time series for rain gauge stations. The inverse distance weighted approach was used to spatially interpolate the point-wise 50-year design storm over the watershed. To illustrate the temporal pattern of the design storm in the watershed, the Pilgrim approach was applied (Pilgrim and Cordery 1975). The storm duration was designed to be roughly equal to the concentration time in the watershed (7 h). The gridded curve number method, MadClark method, recession method, and Lag method were selected for each component of the runoff process as loss method, Transform Method, base flow model, and channel routing, respectively. These methods were selected based on their applicability and limitations, the availability of data, their suitability for the same hydrologic situation and broad acceptability.

Sensitivity analysis of the model parameters was performed to determine the appropriate parameters for calibration of the model. For this purpose, sensitivity analysis was manually performed for the curve number, lag time, storage coefficient, and CNRatio. By doing so, each parameter was changed by 5, 10, and 15%, and the amount of flood hydrograph change in the basin outlet was determined. Then, the model was calibrated semi-manually by Simple-Split Sample Test (Ewen and Parkin 1996). In this method, observational floods are divided into two categories. The model parameters are calibrated with a set of data, then the model validation is performed by implementing the model with the optimized parameters for the second set of data. To evaluate the efficiency of the extracted hydrographs, the statistical indices of root-mean-square error (RMSE), Nash–Sutcliffe coefficient (NSE), and Percent BIAS (PBIAS) are presented in Eqs. 2–4. Where, Q_{obs} represents the observed flow and Q_{sim} represents the computational flow.

$$RMSE = \sqrt{\frac{\sum_{i=1}^{n} \left(Q_{obs} - Q_{sim}\right)^2}{n}} \tag{2}$$

$$NSE = 1 - \left[\frac{\sum_{t=1}^{n} (Q_{obs} - Q_{sim})^2}{\sum_{t=1}^{n} \left(Q_{obs} - \hat{Q}_{obs}\right)^2}\right] \tag{3}$$

$$PBIAS = 100 \times \left[\frac{\sum_{i=1}^{n} (Q_{obs} - Q_{sim})}{\sum_{i=1}^{n} (Q_{obs})} \right] \tag{4}$$

2.4 Multi-Criteria Decision Method by TOPSIS

The TOPSIS is one of the most popular multi-criteria decision models introduced by Wang and Yoon in 1981. This method is based on the fact that the best option should have the minimum distance from the ideal solution (best case) and the maximum distance from the negative ideal (worst case) (Tzeng and Huang 2011). Indicators have both positive and negative aspects. The index that has a positive aspect is profit and the index which has a negative aspect is cost (Chu and Lin 2009). In this study, 11 morphometric indices (Form Factor, Compactness Coefficient, Basin Circularity, Basin Elongation, Drainage density, Ruggedness number, Drainage texture, Stream frequency, Bifurcation ratio, Relief ratio, Shape factor, and Stream length) were used for the multi-criteria decision model.

To use the TOPSIS model, the following steps should be taken: 1. Construct the Primary matrix (Eq. 5), 2. Standardize the evaluation matrix (Eq. 7), 3. Determine the weight of each indicator (in this study the Shannon entropy (Shannon 1948)was used (Eqs. 13–16)). 4. Multiply the standard R_{ij} matrix by its corresponding weight (Wj) (Eq. 7), 5. Determine the best values of the positive ideal solution (A +) and the negative ideal (A-) (Eqs. 8 and 9), 6. Calculate the distance of each option from the positive (di +) and negative (di-) ideals (Eqs. 10 and 11), 7. Calculate the relative proximity (Ai) to the ideal solution (Eq. 12), and 8. rank sub-basins in descending order (Ozdemir and Bird 2009):

$$A_{ij} = \begin{bmatrix} a_{11} & \cdots & a_{1n} \\ \vdots & \vdots & \vdots \\ a_{m1} & \cdots & a_{mn} \end{bmatrix} \tag{5}$$

$$R_{ij} = \frac{a_{ij}}{\sum_{i=1}^{m} a_{ij}} \tag{6}$$

$$V_{ij} = R_{ij} W_j \tag{7}$$

$$A^{+} = \left\{ \left(maxV_{ij} | j \in j\prime \right), \left(minV_{ij} | j \in j\prime \right) | i = 1,2,\ldots,m \right\} = \left\{ V_1^{+}, V_2^{+}, \ldots, V_n^{+} \right\} \tag{8}$$

$$A^{-} = \left\{ \left(minV_{ij} | j \in j\prime \right), \left(maxV_{ij} | j \in j\prime \right) | i = 1,2,\ldots,m \right\} = \left\{ V_1^{-}, V_2^{-}, \ldots, V_n^{-} \right\} \tag{9}$$

$$d_{i+} = \sqrt{\sum_{j=1}^{n} (V_{ij} - V_n^{+})^2 ; i = 1,2,\ldots,m} \tag{10}$$

$$d_{i-} = \sqrt{\sum_{j=1}^{n} (V_{ij} - V_j^{-})^2 ; i = 1,2,\ldots,m} \tag{11}$$

$$cl_{i+} = \frac{d_{i-}}{d_{i+} + d_{i-}}; 0 \le cl_{i+} \le 1; i = 1,2,\ldots,m \tag{12}$$

2.5 Artificial Neural Network (ANN)

2.5.1 Dataset

Since the flood source areas obtained from observational data were not available, the HEC-HMS flood simulation results were used to run the ANN model (Dehghanian et al. 2020). Numerous researchers have confirmed the efficiency of HEC-HMS in determining flood source areas in different conditions (Barbosa et al. 2019; Dehghanian et al. 2020; Ouédraogo et al. 2018; Saghafian et al. 2008; Saghafian and Khosroshahi 2005; Tassew et al. 2019), and according to the simulation results of the rainfall-runoff process in Table 3, hydrological modeling can provide reliable results.

To enhance the performance of the models, it is desired to eliminate elements that have no impact on modeling outcomes and may even impair the models' prediction capacity (Bui et al. 2016). The OneRAttributeEval was used for assessing the parameters for modeling in this study (Holte 1993). OneRAttributeEval uses the OneR classifier to determine the value of an attribute. OneRAttributeEval creates a separate rule for each predictor in the data. The rule with the least overall error is then chosen as the "one rule". The OneRAttributeEval was trained using a tenfold cross-validation methodology in Weka 3.9.5 software. Since it provides larger sigmoid training datasets than the hold-out method (Kim 2009), it delivers a lower estimation of variance (Platt 1999). A greater OneRAttributeEval value indicates that the conditioning factor is more predictive.

The collinearity of the conditioning factors is a feature that most regression analyses are sensitive to (Bai et al. 2011). When two conditioning factors are highly correlated, it is troublesome and could lead to an error in the study. This issue is referred to as multicollinearity. Spearman correlation coefficients (Sedgwick 2012), variance decomposition proportions (Schuerman 2012), conditional index (Belsley 1991), and variance inflation factors (VIF), and tolerances (Dormann et al. 2013) are some of the multicollinearity diagnostics techniques for quantifying factors. In the present study, the Spearman correlation coefficients method was used to test the correlation among the parameters. Spearman's coefficient is a non-parametric measure of statistical dependence between two observational random sequences. It accesses the relationship between sequences where the coefficient can be expressed using a uniform function as follows:

Table 3 Results of calibration and validation events

Flood event		Peak flow(m3/s)		Peak time		Performance indicators		
	Date	Obs	Sim	Obs	Sim	NSE	RMSE	Percent Bias
Calibration	May 11,1991	49.2	48.6	16:00	16:15	0.943	0.2	8.10%
	May 13,1992	74.3	76.7	10:00	10:15	0.798	0.4	13.94%
	Jun 5,1992	92.6	91	1:00	1:15	0.908	0.3	-23.14%
	Feb 21,1999	88.4	84	10:00	10:15	0.973	0.2	-12.34%
Validation	Jun 8,1992	110.6	107.5	16:30	16:30	0.826	0.4	-19.15%
	May 4,2002	58	57.7	0:00	23:30	0.899	0.3	3.73%

$$\rho = 1 - \frac{6\sum d^2}{n(n^2-1)} \tag{17}$$

where ρ represents Spearman's rank correlation coefficient, d is the difference between sequences and n is the number of sequences.

2.5.2 Model Structure

An ANN is a processor made up of neurons that can learn and store information through a training process. The ANN has been widely used in pattern recognition and classification studies (Kawabata and Bandibas 2009). The ANNs can handle nonlinear processes well and is therefore widely used in many disciplines, including flood prediction in hydrology (Tayfur et al. 2018). In order to forecast flood hazard categorization at the cell size, a variety of multilayer perceptron (MLP) networks were used in this study. Watershed characteristic layers served as the ANN model's inputs, while the HEC-HMS simulation of flood hazard categorization served as the model's output. Moreover, the transfer functions for the hidden and output layers were selected as sigmoid tangent and linear, respectively. The Levenberg–Marquardt method was chosen for this study because it is thought to deliver satisfactory outcomes for the majority of the ANN applications (Awchi 2014). One advantage of the ANN model is that it can learn the model through nonlinear and complex relationships. It can also generalize the model and can predict unseen data in the model by understanding the hidden relationship (Band et al. 2020). The ANN algorithms were developed using the following Eqs. by Hagan et al. (1996):

$$net_j^l(t) = \sum_{i=0}^{t} (y_i^{i=1}(t) w_{ji}^l(t)) \tag{18}$$

The net input of the j[th] neuron of layer l and iteration

$$y_j^l(t) = f(net_j^{(l)}(t)) \tag{19}$$

$$f(net) = \frac{1}{1 + e^{(-net)}} \tag{20}$$

$$e_j(t) = c_j(t) - a_j(t) \tag{21}$$

$$\delta_j^l(t) = e_j^l(t) a_j(t)[1 - a_j x(t)] \tag{22}$$

δ factor for the j[th] neuron in the i[th] output layer

$$\delta_j^l(t) = y_j^l(t)[1 - y_j(t)] \sum \delta_j^l(t) w_{kj}^{(l+1)} t \tag{23}$$

δ factor for the j[th] neuron in the i[th] hidden layer

$$w_{ji}^l(t+1) = w_{ji}^l(t) + \alpha \left[w_{ji}^l(t) - w_{ji}^l(t-1) \right] + n\delta_j^l(t) y_j^{(l-1)}(t) \tag{24}$$

where α is the momentum rate and *n* is the learning rate.

The cost function (proportional function) of the i[th] particle can be defined based on the MSE in Eq. 25:

$$MSE = \frac{1}{n}\sum_{i=1}^{n}\left(Y_i - \hat{Y}_i\right)^2 \tag{25}$$

The model efficacy was assessed using statistical criteria for both the training and testing datasets. Model prediction results were evaluated using the statistical measures of Accuracy, Precision, Recall, F1 Score, and AUC (Eqs. 26–30). True Positive (TP) indicates the number of pixels correctly classified as positive predictions, True Negative (TN) indicates the number of pixels correctly classified as negative predictions, and False Positive (FP) and False Negative (FN) indicate the number of pixels incorrectly classified as positive or negative, respectively (Onan 2015).

$$\text{Accuracy} = \frac{\text{TP} + \text{TN}}{\text{TP} + \text{FP} + \text{TN} + \text{FN}} \tag{26}$$

$$\text{Precision} = \frac{\text{TP}}{\text{TP} + \text{FP}} \tag{27}$$

$$\text{Recall} = \frac{\text{TP}}{\text{TP} + \text{FN}} \tag{28}$$

$$\text{F1 score} = 2 \times \frac{\text{Precition} \times \text{Recall}}{\text{Precition} + \text{Recall}} \tag{29}$$

$$\text{AUC} = \frac{\sum \text{TP} + \sum \text{TN}}{\text{P} + \text{N}} \tag{30}$$

where, (Y_i) target value$and\left(\hat{Y}_i\right)$ the predicted output.

3 Results and Discussion

3.1 HEC-HMS

3.1.1 Sensitivity Analysis, Calibration, and Validation of HEC-HMS

The results of the sensitivity analysis for the selected parameters including time of concentration, lag time, storage coefficient, CNratio, and curve number showed that the parameters related to the curve number (Grided curve number and CNratio) have the highest and the storage coefficient has the lowest sensitivity. Since the changes of storage coefficient in the sensitivity analysis stage had a very small effect on the output hydrograph, it was considered constant in the calibration stage and the model calibration was performed with the parameters of time of concentration, lag time, CNratio, and curve number (Fanta and Feyissa 2021). The results of the model calibration and validation are shown in Table 3.

The NSE, RMSE, and PBIAS values were compared with the evaluation levels presented by Barbosa et al. (2019). According to the results from Table 3, the NSE values (0.797- 0.973) are considered very good, the RMSE values (0.2- 0.4) are good and PBIAS values (-23.14%—13.94%) are desirable to very good. The results of the number of errors in Table 3 shows the good performance of the model, which is reasonably accurate compared to other studies (Gharib et al. 2018; Ghavidelfar et al. 2011).

3.1.2 Prioritization and Classification of Sub-basins by HEC-HMS

The amount of runoff produced in each sub-basin was used to determine the source of the flood and the sub-basins were ranked accordingly. Also, after the normalization of the results of the production runoff, the classification map of the sub-basins were categorized into five classes (Obeidat et al. 2021). The results in Fig. 4 show that sub-basins 74, 6, 66, and 53 have the highest amount of runoff and sub-basins 24, 23, 69, and 44 have the lowest amount of production runoff. The map of the flood source areas shows that very high and high classes are located in the North and Northwest of the basin. These sub-basins are characterized by high precipitation and steep slope and are occupied by moderate and poor rangeland. According to Fig. 2e the Northwest of the basin consists of hydrologic group C which indicates a high potential for runoff generation. The southern sub-basins of the basin have low and very low flood hazard due to the relatively low slope, high permeability soils, and medium to good vegetation cover of the pastures (Natarajan and Radhakrishnan 2020).

3.2 Prioritization and Classification of Sub-basins by TOPSIS

The data used in the TOPSIS method included 11 morphometric parameters. The range of changes and weight of each criterion calculated through Shannon entropy method is presented in Table 4. Accordingly, the weight of the parameters varies from 0.009 to 0.197. The logic of Shannon's entropy method is based on the fact that the higher the scatter in the

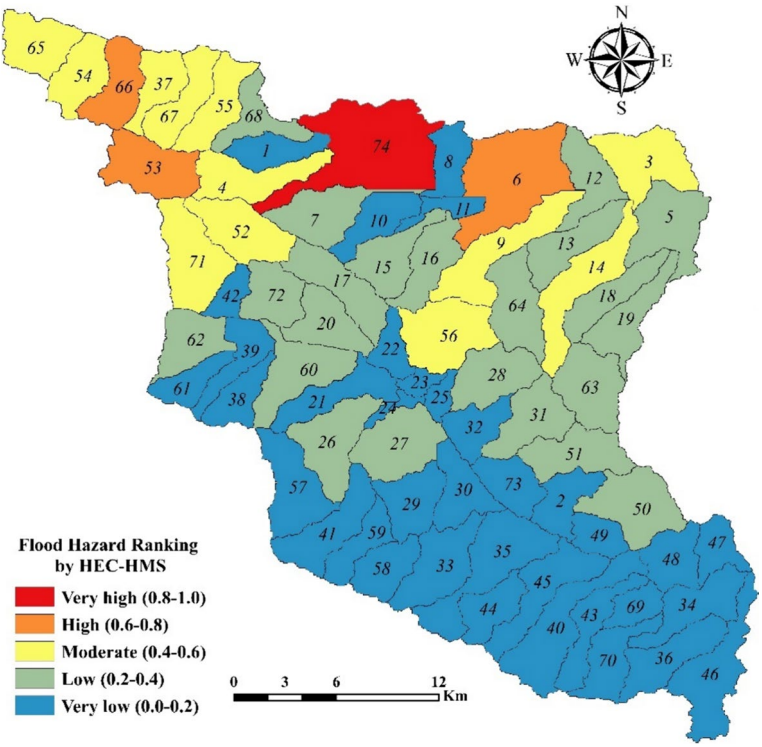

Fig. 4 Flood hazard classification by HEC-HMS model

values of an index, the more important the index. More variation in the values of a variable will lead to lower values of entropy and vice versa. The results of weighting indicate the importance of Br index with a weight of 0.197 and then Li, Ff and Rr indices with weights of 0.188, 0.185 and 0.116, respectively, and Dd as the least effective criterion. From the above parameters, Compactness index(Cc), Elongation(E) and Bifurcation ratio(Br) have a negative effect on runoff generation, while the other parameters have a positive effect.

Sub-basins were prioritized using the TOPSIS method and after normalizing the relative proximity values (cl_{i+}), the sub-basins were classified into 5 flood sensitivity groups. The final classification of flood susceptibility is shown in Fig. 4. In this method, sub-basins 6 and 74, which cover 7% of the basin area are in the Very high class, sub-basins 27 and 35, which constitute 4% of the basin area are in the High class, and 68.2%, 16%, and 4.5% of the basin area are in the Moderate, Low and Very low classes, respectively (Fig. 5). Sub-basins 6 and 74 are classified as Very high class. The main reason behind this include having Maximum Li which has a high weight, and encompassing a large area, and also the many land use changes which have occurred in these sub-basins. Sub-basins 27 and 35, which are in the high risk class, have fair rangelands and dry land agricultural land use. Medium risk areas that cover most parts of the basin are in a wide range of different conditions such as the northwestern areas of the basin which have a mountainous topography with high slope and high rainfall; the vegetation of these areas is medium rangeland and low-density forest and soil hydrological group C and D. In the southwestern regions, the slope is low, the vegetation is of medium rangeland and rain fed agriculture type, and the soil hydrological group is B and C. In general, the sub-basins in this class do not follow a specific trend. These results also apply to the low-risk and safe classes, and the conditions in these sub-basins do not follow a specific pattern.

3.3 Prioritize and classification of sub-basins by the ANN

3.3.1 Considered flood-influencing factors

In order to assess the variables for modeling in the current study, OneRAttributeEval approach and multicollinearity diagnostic method, namely Spearman's correlation coefficient, were chosen. The whole dataset is a matrix which included 1979 lines and each line includes 5 parameters as input and one output. The dataset was divided into two groups of training and testing data with a ratio of 70—30 percent (Khosravi et al. 2019; Tien Bui et al. 2016).

OneRAttributeEval was trained using a tenfold cross-validation method. A higher mean value of OneRAttributeEval (AM) indicates that the conditional factor has more predictive

Table 4 Range of parameter changes, weight of each parameter and its relation with runoff

Parameter	Ff	Cc	Rc	E	Dd	Rn	T	Fs	Br	Rr	Li
Min	0.12	1.59	0.13	0.38	1.89	0.57	3.65	2.99	1.44	0.06	5.64
Max	0.77	2.73	0.39	0.99	3.07	2.71	9.45	6.32	7.69	0.24	90
Variation range	0.66	1.14	0.26	0.61	1.18	2.14	80.5	3.33	6.26	0.18	84.4
STDV	0.17	0.29	0.07	0.15	0.23	0.50	1.07	0.69	1.33	0.04	13.6
Weight	0.185	0.020	0.073	0.05	0.009	0.099	0.041	0.021	0.197	0.116	0.188
Impact on runoff	+	-	+	-	+	+	+	+	-	+	+

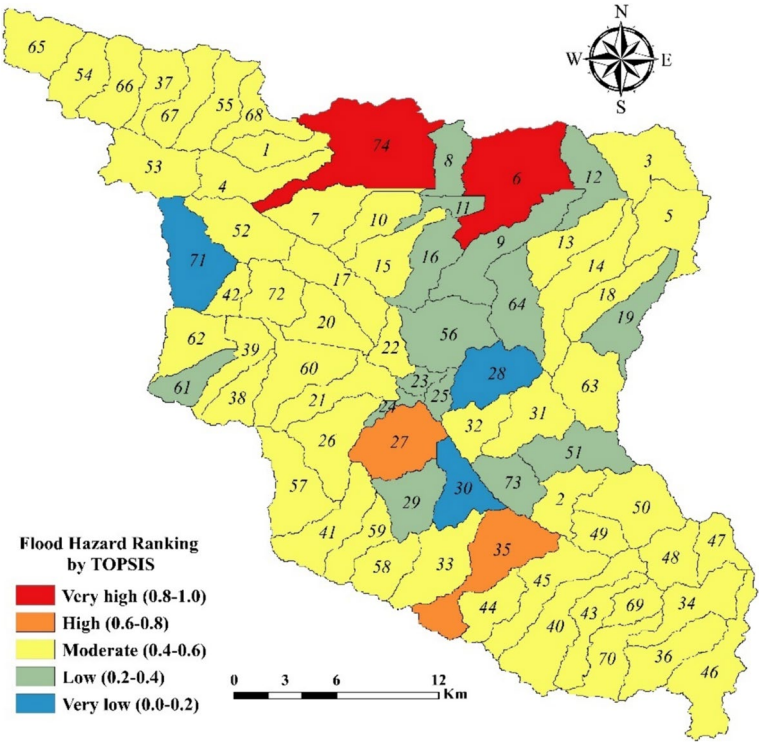

Fig. 5 Flood hazard classification by TOPSIS

ability. The feature selection results show that curve number is the most important factor for flood modeling (AM = 99.6), followed by DEM (AM = 99.46), maximum 50-year daily precipitation (P50) (AM = 99.44), TWI (AM = 99.4) and TRI (AM = 99.2), that indicates the good performance of these parameters in estimating the flood risk classes.

In the present study, Spearman's correlation coefficient method was used to test the correlation between the five input factors and the output. According to the results of multicollinearity diagnostics tests (Table 5), except for the maximum 50-year rainfall (P50) which had a relatively high correlation (-0.713) with the output of the model (Y), none of the parameters had a significant correlation with each other and the output (Y). Since rainfall is actually the most important factor in rainfall-runoff events, it should be considered in prioritizing areas in terms of potential runoff production (Saghafian and Khosroshahi 2005). Therefore, the P50 layer should be used along with the most effective selected variables (Dehghanian et al. 2020).

3.3.2 Model Structure and Performance

The MLP model was constructed with two layers and a number of 5 hidden neurons, batch size 64, learning rate 0.006, momentum 0.3, seed 0, and the number of repetitions 15,000 times and was trained using the training dataset. Using the testing dataset, the model was validated (Table 6). The results show that the model worked perfectly in very high, high and very low classes, and in moderate and low classes with an F1 score of 0.995 and 0.997

Table 5 Parameter correlations

	BasinCN	DEM	P50	TWI	TRI	Y
BasinCN	1.00	0.335	0.158	-0.538	0.323	-0.461
DEM		1.00	-0.034	-0.245	-0.194	-0.029
P50			1.00	-0.426	0.399	-0.713
TWI				1.00	-0.649	0.566
TRI					1.00	-0.296
Y						1.00

and an AUC of 0.999 and 0.997. The overall errors of the model are equal to 0.998, 0.998, 0.998, and 0.999 for Precision, Recall, F1 Score and AUC respectively (Table 6). The results of the testing dataset showed that 99.83% of cells were correctly classified.

The ANN model was subsequently utilized to calculate the flood source areas for all the pixels inside the study area since it surpassed the benchmark models and performed successfully for both the training and validation datasets. These indices were entered to the ArcGIS 10.2 software to create the final flood source maps. The maps were then classified into five categories including very high (3.85%), high (6.15%), moderate (18.6%), low (31.96%), and very low (39.43%) levels of flooding (Fig. 6). These results show that the ANN model was successful in dividing the research region into different hazard classes (Fig. 6).

3.4 Comparison of ANN, HEC-HMS and TOPSIS

The results of the sub-basin classifications in the HEC-HMS hydrological model were compared by the TOPSIS method and the ANN. The results of orrelation, Precision, Recall, F1 score and AUC indices between different methods are presented in Table 7. The results of the error rate between the hydrological model methods and the ANN in Table 7 indicate the good accuracy of the ANN in estimating flood areas. While the error rate in the TOPSIS methods and the ANN indicates the inefficiency of the TOPSIS method as compared to the other two methods. A comparison of the correlation between the TOPSIS method with the hydrological model (0.252) and the ANN (0.233) indicates that there is a significant difference between the two methods. However, the classification results of the hydrological model and the ANN have a significant correlation (0.992). Dehghanian et al. (2020) concluded that the results of the ANN and hydrological model are highly correlated.

Figure 7 shows the percentage of area in each hazard class in different methods. In the methods of hydrological model and the ANN, one sub-basin with an area of 3.8% of the total basin and in the TOPSIS method, two sub-basins with an area of 7% of the total

Table 6 Testing results

Class	Precision	Recall	F1 Score	AUC	NO. Cells
Very high	1.000	1.000	1.000	1.000	22
High	1.000	1.000	1.000	1.000	31
Moderate	0.991	1.000	0.995	0.999	108
Low	1.000	0.995	0.997	0.997	184
Very low	1.000	1.000	1.000	1.000	249
Overall	0.998	0.998	0.998	0.999	594

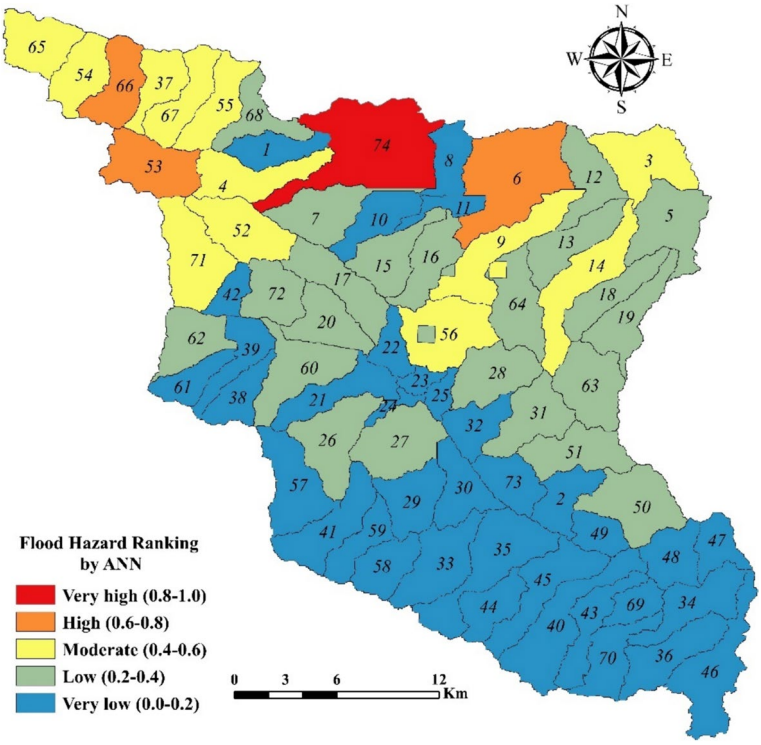

Fig. 6 Flood hazard classification by the ANN

basin are in a Very high class. In the High class in the hydrological model and the ANN, three sub-basins with an area of 57,917 Km^2 (6.15% of the total basin) and in the TOPSIS method, two sub-basins with an area of 38.57 km^2 (4.1% of the total basin) are in this class. The TOPSIS method has classified more than 68% of the basin area (52 sub-basins) in the Moderate class, while in the hydrological model and the ANN 18.64% (12 sub-basins) and 20.24% (13 sub-basins) are in this class, respectively. The hydrological model, the TOPSIS and the ANN have classified 31.92% (22 sub-basins), 16.07% (15 sub-basins) and 30.32% (21 sub-basins) of the total basin area in the low class, respectively. The number and overall area of sub-basins in the very low class were equal in the methods of the hydrological model and the ANN (39.43% and 36 sub-basins), while in the TOPSIS method only three sub-basins with an area of 43.18 km^2 (4.59%) were placed in this class.

Table 7 Comparison of error indices and correlation coefficient(CC) for different methods

	HEC-HMS-TOPSIS	HEC-HMS-ANN	TOPSIS-ANN
Precision	0.268	0.985	0.382
Recall	0.401	0.991	0.255
F1 score	0.254	0.987	0.243
AUC	0.602	0.994	0.527
CC	0.252	0.992	0.233

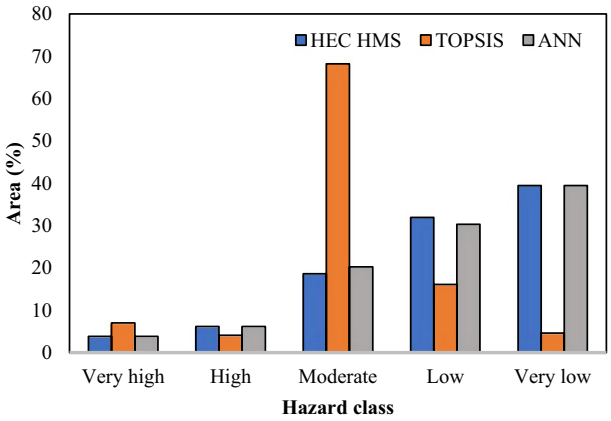

Fig. 7 Percentage of area in each hazard class in different methods

4 Conclusion

The purpose of this research was to investigate and compare the results of three common approaches including HEC-HMS model, the TOPSIS method and the ANNs for determining flood source areas. The results of the classification of sub-basins by HEC-HMS showed that sub-basins 74 and 6 have a high flood risk and sub-basins 69, 70, and 40 have a low flood risk. The results of classification by different methods as well as the results of the correlation and error indicate the difference in the flood classification of the basin. Since the ANN model has simulated the HEC-HMS classifications very accurately (Fig. 6), it can be concluded that this model has performed better than the TOPSIS multi-criteria decision-making method and is more efficient. Also, the results of the degree of correlation of the results presented in Table 7 indicate no meaningful correlation between the results of the TOPSIS classification and the hydrological model. Therefore, it can be concluded that the ANN model performed better as compared to the TOPSIS multi-criteria decision-making method and can be used in other areas with similar hydrological and morphological characteristics.

Acknowledgements The authors gratefully acknowledge the funding support of Ferdowsi University of Mashhad. We also appreciate the assistance of Dr. Atiyeh Kamyabi Gol from Linguistics Department, Ferdowsi University of Mashhad for the language editing and proofreading.

Authors' contribution All authors contributed to the study conception and design. Material preparation and data collectionwere performed by EM. MA and MT participated in the analysis and interpretation of the results. The first draft of the manuscript was written by EM and AS and all authors commented on previous versions of the manuscript. All authors read and approved the final manuscript.

Funding This work was supported by the funding support of Ferdowsi University of Mashhad, Iran [Grant number: 51950].

Data Availability All data, models, or codes that support the findings of this study are available from the corresponding author upon reasonable request.

Code availability All data, models, or codes that support the findings of this study are available from the corresponding author upon reasonable request.

Declarations

Ethics approval Not applicable.

Consent to participate Not applicable.

Consent for publication All authors have participated the manuscript and agree with submission to Water Resources Management.

Conflicts of interest The authors declare no conflict of interest.

References

Abdulkareem JH, Sulaiman WNA, Pradhan B, Jamil NR (2018) Relationship between design floods and land use land cover (LULC) changes in a tropical complex catchment. Arab J Geosci 11(14):376

Ajjur SB, Mogheir YK (2020) Flood hazard mapping using a multi-criteria decision analysis and GIS (case study Gaza Governorate, Palestine). Arab J Geosci 13:1–11

Awchi TA (2014) River discharges forecasting in northern Iraq using different ANN techniques. Water Resours Manag 28:801–814

Bai T, Tahmasebi P (2023) Graph neural network for groundwater level forecasting. J Hydrol 616:128792

Bai S, Lü G, Wang J, Zhou P, Ding L (2011) GIS-based rare events logistic regression for landslide-susceptibility mapping of Lianyungang China. Environ Earth Sci 62:139–149

Bailey RG (1976) Ecoregions of the United States. US Forest Service, Ogden, Utah p 1

Band SS, Janizadeh S, Chandra Pal S, Saha A, Chakrabortty R, Shokri M, Mosavi A (2020) Novel ensemble approach of deep learning neural network (DLNN) model and particle swarm optimization (PSO) algorithm for prediction of gully erosion susceptibility. Sensors 20(19):5609

Barbosa J, Fernandes A, Lima A, Assis L (2019) The influence of spatial discretization on HEC-HMS modelling: a case study. Intl J Hydrol 3(5):442–449

Belsley DA (1991) A guide to using the collinearity diagnostics. Comput Sci Econ Manag 4(1):33–50

Belton V, Stewart T (2002) Multiple criteria decision analysis: an integrated approach. Springer Science & Business Media, Wiley, New York

Beven K (2001) Rainfall-runoff modelling: The Primer, John Wiley and Sons Press. University of London Egham, Surrey, Department of Geography Royal Holloway

Beven KJ (2011) Rainfall-runoff modelling: the primer. John Wiley & Sons

Bolt BA, Horn WL, MacDonald GA, Scott RF (2013) Geological hazards: earthquakes-tsunamis-volcanoes-avalanches-landslides-floods. Springer Science & Business Media, New York

Bonell M, Purandara B, Venkatesh B, Krishnaswamy J, Acharya H, Singh U, Jayakumar R, Chappell N (2010) The impact of forest use and reforestation on soil hydraulic conductivity in the Western Ghats of India: Implications for surface and sub-surface hydrology. J Hydrol 391(1–2):47–62

Brans JP, Mareschal B, Figueira J, Greco S (2005) Multiple criteria decision analysis: state of the art surveys. Springer Science & Business Media, New York

Bui DT, Pradhan B, Nampak H, Bui Q-T, Tran Q-A, Nguyen Q-P (2016) Hybrid artificial intelligence approach based on neural fuzzy inference model and metaheuristic optimization for flood susceptibilitgy modeling in a high-frequency tropical cyclone area using GIS. J Hydrol 540:317–330

Cabrera JS, Lee HS (2019) Flood-prone area assessment using GIS-based multi-criteria analysis: A case study in Davao Oriental. Philippines Water 11(11):2203

Chu T-C, Lin Y-C (2009) An interval arithmetic based fuzzy TOPSIS model. Expert Syst Appl 36(8):10870–10876

Costache R, Arabameri A, Costache I, Crăciun A, Pham BT (2022) New Machine Learning Ensemble for Flood Susceptibility Estimation. Water Resour Manage 36(12):4765–4783. https://doi.org/10.1007/s11269-022-03276-0

CrED U (2015) The human cost of weather-related disasters, 1995–2015. United Nations, Geneva

Dadrasajirlou Y, Karami H, Mirjalili S (2023) Using AHP-PROMOTHEE for selection of best Low-Impact Development designs for urban flood mitigation. Water Resour Manage 37(1):375–402

Dawson C, Wilby R (2001) Hydrological modelling using artificial neural networks. Prog Phys Geogr 25(1):80–108

Dehghanian N, Nadoushani SSM, Saghafian B, Akhtari R (2019) Performance evaluation of a fuzzy hybrid clustering technique to identify flood source areas. Water Resourc Manag 33:4621–4636
Dehghanian N, Nadoushani SM, S., Saghafian, B. and Damavandi, M.R. (2020) Evaluation of coupled ANN-GA model to prioritize flood source areas in ungauged watersheds. Hydrol Res 51(3):423–442
Dong N, Guan W, Cao J, Zou Y, Yang M, Wei J, Chen L, Wang H (2023) A hybrid hydrologic modelling framework with data-driven and conceptual reservoir operation schemes for reservoir impact assessment and predictions. J Hydrol 619:129246
Dormann CF, Elith J, Bacher S, Buchmann C, Carl G, Carré G, Marquéz JRG, Gruber B, Lafourcade B, Leitão PJ (2013) Collinearity: a review of methods to deal with it and a simulation study evaluating their performance. Ecography 36(1):27–46
dos Santos JC, Lyra GB, Abreu MC, Andrade CD, Moster C, Cunha-Zeri G, Zeri M (2023) Flood-prone areas based on physiographic indices and multi-criteria assessment for the basins of Ubatuba, on the mountainous North Coast of São Paulo State Brazil. Environ Earth Sci 82(21):517. https://doi.org/10.1007/s12665-023-11207-4
Ewen J, Parkin G (1996) Validation of catchment models for predicting land-use and climate change impacts. 1 Method. J Hydrol 175(1–4):583–594
Fanta SS, Feyissa TA (2021) Performance evaluation of HEC-HMS model for continuous runoff simulation of Gilgel Gibe watershed, Southwest Ethiopia. J Water Land Dev 50:85–97
Gharib M, Motamedvaziri B, Ahmadi H, Ghermezcheshmeh B (2018) Evaluation of ModClark model for simulating rainfall-runoff in Tangrah watershed, Iran. Appl Ecol Environ Res 16(2):1053–1068. https://doi.org/10.15666/aeer/1602_10531068
Ghavidelfar S, Alvankar SR, Razmkhah A (2011) Comparison of the lumped and quasi-distributed Clark runoff models in simulating flood hydrographs on a semi-arid watershed. Water Resourc Manag 25:1775–1790
Ghobadi M, Ahmadipari M (2024) Enhancing Flood Susceptibility Modeling: a Hybrid Deep Neural Network with Statistical Learning Algorithms for Predicting Flood Prone Areas. Water Resour Manage. https://doi.org/10.1007/s11269-024-03770-7
Ha J, Kang J (2022) Assessment of flood-risk areas using random forest techniques: Busan Metropolitan City. Nat Hazards 111:2407–2429. https://doi.org/10.1007/s11069-021-05142-5
Hadian S, Afzalimehr H, Soltani N, Tabarestani ES, Karakouzian M, Nazari-Sharabian M (2022) Determining flood zonation maps, using new ensembles of multi-criteria decision-making, bivariate statistics, and artificial neural network. Water 14(11):1721
Hagan MT, Demuth HB, Beale M (1996) Neural network design. PWS Publishing Co., Boston
Holte RC (1993) Very simple classification rules perform well on most commonly used datasets. Mach Learn 11:63–90
Hong Y, Abdelkareem M (2022) Integration of remote sensing and a GIS-based method for revealing prone areas to flood hazards and predicting optimum areas of groundwater resources. Arab J Geosci 15(1):114
Hong H, Tsangaratos P, Ilia I, Liu J, Zhu AX, Chen W (2018) Application of fuzzy weight of evidence and data mining techniques in construction of flood susceptibility map of Poyang County, China. Sci Total Environ 625:575–588
Hwang CL, Yoon K (1981) Methods for multiple attribute decision making. Multiple attribute decision making: methods and applications a state-of-the-art survey. Springer, Berlin, pp 58–191
Islam ARMT, Talukdar S, Mahato S, Kundu S, Eibek KU, Pham QB, Kuriqi A, Linh NTT (2021) Flood susceptibility modelling using advanced ensemble machine learning models. Geosci Front 12(3):101075
Islam ARMT, Bappi MMR, Alqadhi S, Bindajam AA, Mallick J, Talukdar S (2023) Improvement of flood susceptibility mapping by introducing hybrid ensemble learning algorithms and high-resolution satellite imageries. Nat Hazards 119(1):1–37. https://doi.org/10.1007/s11069-023-06106-7
Kawabata D, Bandibas J (2009) Landslide susceptibility mapping using geological data, a DEM from ASTER images and an Artificial Neural Network (ANN). Geomorphology 113(1–2):97–109
Khosravi K, Shahabi H, Pham BT, Adamowski J, Shirzadi A, Pradhan B, Dou J, Ly H-B, Gróf G, Ho HL (2019) A comparative assessment of flood susceptibility modeling using multi-criteria decision-making analysis and machine learning methods. J Hydrol 573:311–323
Kim JH (2009) Estimating classification error rate: Repeated cross-validation, repeated hold-out and bootstrap. Comput Stat Data Anal 53(11):3735–3745
Koya SR, Giron NV, Rojas M, Mantilla R, Harvey K, Ceynar D, Quintero F, Krajewski WF, Roy T (2023) Applicability of a flood forecasting system for Nebraska watersheds. Environ Model Softw 164:105693
Liu G, Ouyang S, Qin H, Liu S, Shen Q, Qu Y, Zheng Z, Sun H, Zhou J (2023) Assessing spatial connectivity effects on daily streamflow forecasting using Bayesian-based graph neural network. Sci Total Environ 855:158968

Loucks DP, Van Beek E (2017) Water resource systems planning and management: An introduction to methods, models, and applications. Springer
Luu C, Bui QD, Costache R, Nguyen LT, Nguyen TT, Van Phong T, Van Le H, Pham BT (2021) Flood-prone area mapping using machine learning techniques: A case study of Quang Binh province Vietnam. Nat Haz 108(3):3229–3251
Maghsood FF, Moradi H, Massah Bavani AR, Panahi M, Berndtsson R, Hashemi H (2019) Climate change impact on flood frequency and source area in northern Iran under CMIP5 scenarios. Water 11(2):273
McCulloch WS, Pitts W (1943) A logical calculus of the ideas immanent in nervous activity. Bull Mathematical Biophys 5:115–133
Mitra R, Das J (2023) A comparative assessment of flood susceptibility modelling of GIS-based TOPSIS, VIKOR, and EDAS techniques in the Sub-Himalayan foothills region of Eastern India. Environ Sci Pollut Res 30(6):16036–16067
Mohseni U, Muskula SB (2023) Rainfall-runoff modeling using artificial neural network—a case study of purna sub-catchment of Upper Tapi Basin India. Environ Sci Proc 25(1):1
Mukherjee F, Singh D (2020) Detecting flood prone areas in Harris County: A GIS based analysis. GeoJournal 85(3):647–663
Natarajan S, Radhakrishnan N (2020) An integrated hydrologic and hydraulic flood modeling study for a medium-sized ungauged urban catchment area: A case study of Tiruchirappalli City Using HEC-HMS and HEC-RAS. J Instit Eng (India) Series A 101:381–398
Obeidat M, Awawdeh M, Al-Hantouli F (2021) Morphometric analysis and prioritisation of watersheds for flood risk management in Wadi Easal Basin (WEB), Jordan, using geospatial technologies. J Flood Risk Manag 14(2):e12711. https://doi.org/10.1111/jfr3.12711
Onan A (2015) A fuzzy-rough nearest neighbor classifier combined with consistency-based subset evaluation and instance selection for automated diagnosis of breast cancer. Expert Syst Appl 42(20):6844–6852
Osei BK, Ahenkorah I, Ewusi A, Fiadonu EB (2021) Assessment of flood prone zones in the Tarkwa mining area of Ghana using a GIS-based approach. Environ Chall 3:100028
Ouédraogo WAA, Raude JM, Gathenya JM (2018) Continuous modeling of the Mkurumudzi River catchment in Kenya using the HEC-HMS conceptual model: Calibration, validation, model performance evaluation and sensitivity analysis. Hydrology 5(3):44
Ozdemir H, Bird D (2009) Evaluation of morphometric parameters of drainage networks derived from topographic maps and DEM in point of floods. Environ Geol 56(7):1405–1415
Pappenberger F, Matgen P, Beven KJ, Henry J-B, Pfister L (2006) Influence of uncertain boundary conditions and model structure on flood inundation predictions. Adv Water Resourc 29(10):1430–1449
Pham BT, Luu C, Van Phong T, Nguyen HD, Van Le H, Tran TQ, Ta HT, Prakash I (2021) Flood risk assessment using hybrid artificial intelligence models integrated with multi-criteria decision analysis in Quang Nam Province Vietnam. J Hydrol 592:125815
Pilgrim DH, Cordery I (1975) Rainfall temporal patterns for design floods. J Hydraul Div 101(1):81–95
Platt J (1999) Probabilistic outputs for support vector machines and comparisons to regularized likelihood methods. Adv Large Margin Classifiers 10(3):61–74
Rahman M, Chen N, Islam MM, Mahmud GI, Pourghasemi HR, Alam M, Rahim MA, Baig MA, Bhattacharjee A, Dewan A (2021) Development of flood hazard map and emergency relief operation system using hydrodynamic modeling and machine learning algorithm. J Clean Prod 311:127594
Roy S, Bose A, Chowdhury IR (2021) Flood risk assessment using geospatial data and multi-criteria decision approach: a study from historically active flood-prone region of Himalayan foothill India. Arab J Geosci 14(11):999
Saaty T (1980) The Analytic Hierarchy Process (AHP) for decision making. In: Proceedings of the Kobe, Kobe, Japan, pp 1–69
Sadiq R, Akhtar Z, Imran M, Ofli F (2022) Integrating remote sensing and social sensing for flood mapping. Remote Sens Appl: Soc Environ 25:100697
Saghafian B, Khosroshahi M (2005) Unit response approach for priority determination of flood source areas. J Hydrol Eng 10(4):270–277
Saghafian B, Farazjoo H, Bozorgy B, Yazdandoost F (2008) Flood intensification due to changes in land use. Water Resour Manage 22:1051–1067
Schuerman JR (2012) Multivariate analysis in the human services. Springer Science & Business Media, New York
Sedgwick PM (2012) Pearson's correlation coefficient. BMJ: Br Med J 345:e4483. https://doi.org/10.1136/bmj.e4483
Shannon CE (1948) A mathematical theory of communication. Bell Syst Tech J 27(3):379–423
Sharma TPP, Zhang J, Koju UA, Zhang S, Bai Y, Suwal MK (2019) Review of flood disaster studies in Nepal: A remote sensing perspective. Intl J Disast Risk Reduct 34:18–27

Singh A, Dawson D, Trigg M, Wright N (2021) A review of modelling methodologies for flood source area (FSA) identification. Nat Hazards 107:1047–1068

Solaimani K, Shokrian F, Darvishi S (2023) An Assessment of the Integrated Multi-Criteria and New Models Efficiency in Watershed Flood Mapping. Water Resour Manage 37(1):403–425. https://doi.org/10.1007/s11269-022-03380-1

Solin L, Skubincan P (2013) Flood risk assessment and management: review of concepts, definitions and methods. Geogr J 65:23–44

Soomro SEH, Hu C, Boota MW, Ahmed Z, Chengshuai L, Zhenyue H, Xiang L, Soomro MHAA (2022) River Flood Susceptibility and Basin Maturity Analyzed Using a Coupled Approach of Geo-morphometric Parameters and SWAT Model. Water Resourc Manag 36(7):2131–2160. https://doi.org/10.1007/s11269-022-03127-y

Syifa M, Park SJ, Achmad AR, Lee C-W, Eom J (2019) Flood mapping using remote sensing imagery and artificial intelligence techniques: a case study in Brumadinho, Brazil. J Coast Res 90:197–204

Tassew BG, Belete MA, Miegel K (2019) Application of HEC-HMS model for flow simulation in the Lake Tana basin: The case of Gilgel Abay catchment, upper Blue Nile basin Ethiopia. Hydrology 6(1):21

Tayfur G, Singh VP, Moramarco T, Barbetta S (2018) Flood hydrograph prediction using machine learning methods. Water 10(8):968

Tien Bui D, Tuan TA, Klempe H, Pradhan B, Revhaug I (2016) Spatial prediction models for shallow landslide hazards: a comparative assessment of the efficacy of support vector machines, artificial neural networks, kernel logistic regression, and logistic model tree. Landslides 13:361–378

Tzeng G-H, Huang J-J (2011) Multiple attribute decision making: methods and applications. CRC Press

Van Loon AF (2015) Hydrological drought explained. Wiley Interdiscip Rev Water 2(4):359–392

Viviroli D, Dürr HH, Messerli B, Meybeck M, Weingartner R (2007) Mountains of the world, water towers for humanity: typology, mapping, and global significance. Water Resour Res 43:W07447. https://doi.org/10.1029/2006WR005653

Wang Z, Lai C, Chen X, Yang B, Zhao S, Bai X (2015) Flood hazard risk assessment model based on random forest. J Hydrol 527:1130–1141

Wijesinghe W, Mishra PK, Tripathi S, Abdelrahman K, Tiwari A, Fnais MS (2023) Integrated Flood Hazard Vulnerability Modeling of Neluwa (Sri Lanka) Using Analytical Hierarchy Process and Geospatial Techniques. Water 15(6):1212

Xu Y, Chen Y, Ren Y, Tang Z, Yang X, Zhang Y (2023) Attribution of Streamflow Changes considering spatial contributions and driver interactions based on Hydrological modeling. Water Resour Manage 37(5):1859–1877

Zohourian B, Hosseini SM (2023) Determining flood source areas in watersheds using data-driven models and a geographic information system. Hydrol Sci J 68(10):1443–1459. https://doi.org/10.1080/02626667.2023.2220885